

Crustal thickness variations across the Colorado Rocky Mountains from teleseismic receiver functions

Anne F. Sheehan,¹ Geoffrey A. Abers,^{2,3} Craig H. Jones,¹ and Arthur L. Lerner-Lam²

Abstract. Variations in crustal thickness from the Great Plains of Kansas, across the Colorado Rocky Mountains, and into the eastern Colorado Plateau are determined by receiver function analysis of broadband teleseismic *P* waveforms recorded during the 1992 Rocky Mountain Front Program for Array Seismic Studies of the Continental Lithosphere (PASSCAL) experiment. The receiver functions are calculated using a time domain deconvolution approach and are interpreted in terms of a single crustal layer, with thickness determined by a grid-search comparison of observed receiver functions with synthetics. The average crustal thicknesses determined by these methods are Kansas Great Plains, 43.8 ± 0.4 km; Colorado Great Plains, 49.9 ± 1.2 km; Colorado Rocky Mountains, 50.1 ± 1.3 km; and northeast Colorado Plateau, 43.1 ± 0.9 at latitudes of 38° – 40° N. The main variations in crustal thickness that we observe are between the Kansas Great Plains and the Colorado Great Plains and between the Rocky Mountains and the Colorado Plateau. There is not a significant crustal thickness difference between the Colorado Great Plains and the Colorado Rocky Mountains. Together with gravity data and mass balance calculations, these results are incompatible with the hypothesis that the compensation of the Rocky Mountains relative to the Great Plains is accommodated purely by an Airy-type crustal root or any other mechanism that restricts compensation solely to the crust and requires significant support for the excess topography of the Rocky Mountains to come from the mantle. Models with a rigid elastic plate may match receiver function estimates of crustal thickness but underpredict the amplitude of the gravity low over the Rockies. Our favored model includes lateral variations in crustal velocities obtained from refraction studies and crustal thickness variations constrained by the receiver functions. These models indicate that there is a profound transition in mantle density structure near the eastern range front.

Introduction

Over the past hundred million years, the western United States has deformed in dramatic fashion. Throughout most of Mesozoic time a volcanic arc was active along the present Sierra Nevada and several fold-and-thrust belts developed to the east. In the late Cretaceous, volcanism ceased in the Sierra Nevada and the locus of deformation shifted eastward, where the style of contraction was thick-skinned rather than thin-skinned and is termed the Laramide orogeny [Burchfiel *et al.*, 1992]. As the Laramide orogeny waned in the early Cenozoic, volcanic activity migrated westward from the Rocky Mountains [Lipman, 1992]. Tectonic relief acquired during the Laramide in the Rocky Mountains was subsequently beveled down to a relatively gentle surface [Epis and Chapin, 1975; Dickinson *et al.*, 1988]. Regional uplift of about 2 km in late Cenozoic time has been suggested [Epis and Chapin, 1975; Eaton, 1986, 1987], but the paleontological corroboration for this inference [MacGinitie, 1953; Axelrod and Bailey, 1976] has been challenged and the uplift might be late Eocene [Gregory and Chase, 1992, 1994].

These events have spawned provocative explanations. While the fold-and-thrust belts in and slightly east of the modern Basin and Range seem compatible with “normal” contractile plate margins, the thick-skinned Laramide orogeny, far from a plate boundary, has been difficult to understand. One popular hypothesis is that the geometry of the subducting slab changed in late Mesozoic time, becoming subhorizontal and extending to the eastern edge of the modern Rockies [e.g., Lipman *et al.*, 1971; Bird, 1984]. This in turn has led to the inference that there has been wholesale transport of crust and upper mantle from west to east [Bird, 1984, 1988]. In this particular model, the elevation of the High Plains and the Rocky Mountains is due to an increase in the crustal thickness by lower-crustal flow during the Laramide. Others have compared the shape of the overall uplift to that of a mid-ocean ridge and inferred that the elevations are thermally supported from the mantle [e.g., Eaton, 1987], possibly reflecting the removal of the doubled thickness of lithosphere in the Cenozoic [Bird, 1984]. An entirely different hypothesis is that there was not a horizontal slab beneath North America, at least not one transmitting forces into the lithosphere, and that the Laramide reflects transmission of stress from the plate margin eastward through the lithosphere itself [Molnar and Lyon-Caen, 1988; Livaccari, 1991].

A critical problem in understanding the tectonics of the western United States is to separate the contribution of crust and mantle buoyancy to the elevation of the region. In this paper, we place constraints on the support of the topography by determining relative variations in crustal thickness across the Great Plains, Rocky Mountains, and Colorado Plateau and,

¹Cooperative Institute for Research in Environmental Sciences and Department of Geological Sciences, University of Colorado, Boulder.

²Lamont-Doherty Earth Observatory of Columbia University, Palisades, New York.

³Now at Department of Geology, University of Kansas, Lawrence.

Copyright 1995 by the American Geophysical Union.

combined with the assumption of regionally local isostasy, determine the contribution of the upper mantle to the modern elevation of these provinces. Based upon our observations, we suggest that about half of the compensation of the excess 2 km of elevation of the Rocky Mountains relative to the Great Plains is in the mantle, rather than in the crust.

Before the recent Rocky Mountain Front Program for Array Seismic Studies of the Continental Lithosphere (PASSCAL) experiment, the only detailed information available on the crustal and upper mantle structure of the Rocky Mountains was from a handful of refraction profiles shot in the 1960s. These profiles generally indicated that the crust was about 45–50 km thick with crustal P wave velocities from 6.2 to 6.5 km/s [Braile et al., 1989; Prodehl and Lipman, 1989]. P_n velocities are generally 7.8–8.0 km/s except near the Rio Grande Rift [Braile et al., 1989]. The Rocky Mountains have been inferred to lie at the eastern edge of the region having a “tectonic North America” shear wave velocity structure [Grand and Helmburger, 1984].

The Rocky Mountain Front experiment consisted of a two-phase deployment of seismometers: a reconnaissance phase in 1991 consisting of eight digital broadband three-component seismic stations located in an east-west linear array across the

state of Colorado at a latitude of roughly 39.3°N, and, in 1992, a deployment of 30 broadband (CMG3-ESP and STS2) seismometers distributed throughout Colorado and extending into eastern Utah and western Kansas (Figure 1). The data used here were recorded continuously at 10 samples per second. The array spans three major physiographic provinces: the Great Plains, the Rocky Mountains, and the Colorado Plateau. We analyze teleseismic P waveforms recorded during the experiment in order to constrain crustal structure beneath the array.

Methods and Results

Time Domain Deconvolution for Receiver Functions

Several investigators have shown that the wave train of the teleseismic P arrival can be interpreted in terms of reflections and transmissions of mode-converted waves at discrete boundaries beneath the recording station [e.g., Phinney, 1964; Langston, 1977, 1979, 1981, 1989; Owens et al., 1984, 1987, 1988; Owens and Crosson, 1988]. These techniques regard the recorded signal as a convolution of a source-time function, an instrument response, and a velocity structure, or “receiver”

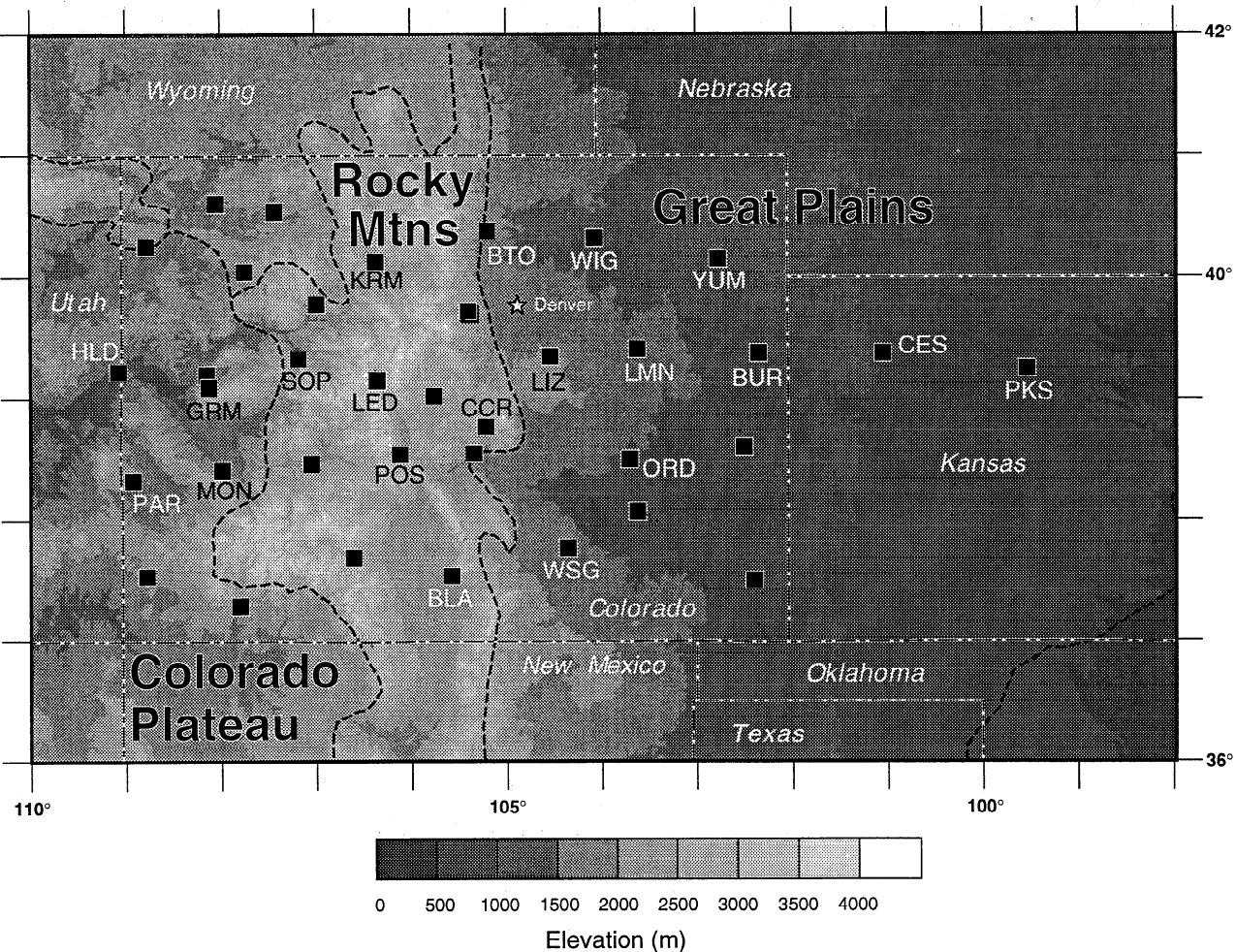


Figure 1. Seismograph stations of Rocky Mountain Front PASSCAL experiment on gray-shaded map of topographic relief, 500-m contour interval. Squares indicate station locations; stations labeled with station name are used in this study. White dashed lines define state boundaries, black dashed lines define physiographic provinces.

function. The primary underlying assumption of this technique is that compared to the direct arrival, P -to- S conversions from discontinuities beneath the receiver are much weaker on the vertical component seismogram $v(t)$ than on the radial component $r(t)$. Therefore $v(t)$ can be used as an estimate of the P source function incident at the base of the crust along with P reverberations, and P -to- S conversions are isolated by the deconvolution of $v(t)$ from $r(t)$.

We employ a time domain deconvolution approach for the determination of teleseismic receiver functions. In the approach used here, the convolutional relationship between the vertical and radial components of one or more seismograms is treated as an invertible system of time domain equations for parameters of the receiver function. The approach is similar to that of *Sipkin and Lerner-Lam* [1992] and *Abers et al.* [1995] and is summarized here.

Let the vertical component of the P waveform be represented by $v(t)$ and the radial component be represented by $r(t)$. We seek to find that function $f(t)$ (the receiver function) which, when convolved with $v(t)$, best reproduces $r(t)$. The linear convolutional relationship between $v(t)$ and $r(t)$ takes the form

$$\begin{aligned} r(t) &= v(t) * f(t) \\ &= \int_{-\infty}^{\infty} v(t-\tau) f(\tau) d\tau. \end{aligned} \quad (1)$$

We assume that $f(t)$ is causal, i.e., that there are no P -to- S conversions before the initial P wave arrival and that all waveforms are adequately sampled by discrete time series.

Most previous solutions to the receiver function problem performed the deconvolution for $f(t)$ by discrete Fourier transform techniques. Although the deconvolution is formally a well-posed inversion, in practice, band-limited and nonstationary seismic signals make such deconvolutions numerically ill-conditioned [e.g., *Sipkin and Lerner-Lam*, 1992; *Gurrola et al.*, 1994, 1995]. Spectral deconvolution techniques require stabilization to overcome the inherently unstable nature of the deconvolution (e.g., water level [*Clayton and Wiggins*, 1976]). An alternative approach is to treat equation (1) as a time domain inverse problem. In the time domain approach, stabilization is accomplished with a damping parameter rather than the water level parameter commonly used in spectral deconvolution. Because the damping parameter affects small eigenvalues the most in the inversion, poorly constrained parts of the receiver function are most affected by stabilization.

In the derivation below, seismograms $r(t)$ and $v(t)$ are denoted r_k and v_k , vectors with values r_k^i and v_k^i corresponding to samples of the k th seismograms at time t_i ($i = 1, 2, \dots, n_k$). Under the assumptions above, equation (1) is represented by the summation

$$r_k^i = \sum_{j=0}^i v_k^{i-j} f^j \quad (2)$$

where f^j is the j th point in the unknown receiver function. For each pair of seismograms $\{v_k, r_k\}$, equation (2) provides n_k linear equations for m values in f^j . Assuming that f is the same for a suite of k events, equation (2) can be represented as a system of equations to be solved for f

$$\begin{vmatrix} \mathbf{r}_1 \\ \mathbf{r}_2 \\ \vdots \\ \mathbf{r}_K \end{vmatrix} = \begin{vmatrix} G_1 \\ G_2 \\ \vdots \\ G_K \end{vmatrix} \mathbf{f} \quad (3)$$

or

$$\mathbf{r} = G\mathbf{f}.$$

The vector \mathbf{r} has the radial component seismograms for one or more events. If desired, multiple seismograms can go into this vector sequentially, rather than performing "stacks," provided that the seismograms are from events at similar distances and azimuths. The matrix G contains the vertical component seismogram(s) in convolutional (Toeplitz) form

$$G_k = \begin{vmatrix} v_k^0 & 0 & . & 0 \\ v_k^1 & v_k^0 & . & . \\ \vdots & \vdots & \vdots & \vdots \\ v_k^{n_k} & v_k^{n_k-1} & . & v_k^{n_k-m} \end{vmatrix} \quad (4)$$

Equation (3) is solved using a damped least squares inversion for \mathbf{f} .

Modeling of Receiver Functions by Grid Search Techniques

Radial receiver functions are estimated using the time domain techniques for each event-station pair, with seismogram length of 40 s and receiver function length equal to 30 s (sample rate 10 samples per second). After deconvolution the receiver functions are padded with zeros to 50 s to reduce the possibility of crustal solutions which produce large reverberations shortly after the 30 s window, where little signal is observed. Synthetic receiver functions for a suite of plausible crustal thicknesses are sequentially tested to find the crustal thickness which gives the minimum root-mean-square difference between the observed receiver function and the corresponding synthetic. These synthetic receiver functions are generated using a plane layered model, with the thickness of the crustal layer differing incrementally for each calculation. The grid-search technique allows visualization of the trade-offs inherent in receiver function inversions in order to select the best model. We feel that with this technique we can utilize the most robust features of the receiver function such as time of Moho P -to- S phase conversions to determine first-order structures in a stable way, with readily analyzable trade-offs between a small number of parameters. The usual alternative of solving for large numbers of free velocity parameters often leads to problems of nonuniqueness [*Ammon et al.*, 1990] that require much more effort to quantify and convey. Also, because we are interested in variations in crustal thickness, it is advantageous to utilize techniques in which crustal thickness is solved for directly from observations. A summary of details of the trade-offs between various parameters is given in the appendix.

Seismograms from 12 teleseismic events of $m_b > 5.5$ recorded during the Rocky Mountain Front deployment were used

Earthquakes used in Receiver Function study

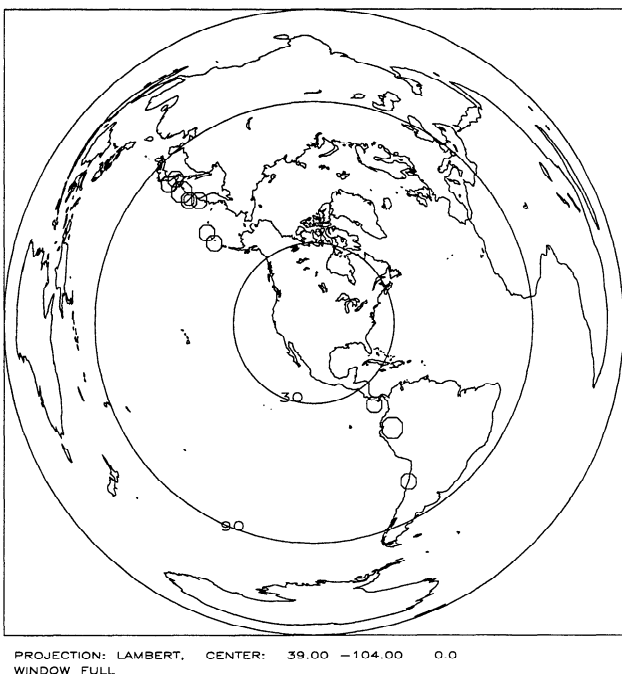


Figure 2. Distribution of earthquakes used in receiver function study. Event symbols scaled by magnitude. Circles of radius 30° and 90° are shown, centered on 39°N, 104°W. Lambert projection.

in this study (Figure 2). The source-receiver separation typically used in receiver function studies ranges from 30° to 90°, where rays bottom in the lower mantle. The events used in this study fell in the epicentral distance range of 38° to 83°. The earthquakes used are located at northwestern (Aleutians,

Kuriles, Honshu) and southeastern (South America) backazimuths from the recording stations.

The receiver functions are interpreted in terms of a single-layer crust in order to determine gross crustal thickness variations across the Rocky Mountain Front. The main features modeled are the first P -to- S conversion at the base of the crust (Ps) and the reverberation $PpPmS$ [Owens *et al.*, 1987]. The Ps phase is a robust feature of the observed receiver functions and provides a strong constraint on travel time to the Moho. A constant crustal P wave velocity of 6.5 km/s was assumed, based on compilations from refraction studies in the region [Braile *et al.*, 1989; Prodehl and Lipman, 1989]. The S wave velocity value was obtained assuming a Poisson's ratio of 0.25, resulting in crustal S wave velocity of 3.76 km/s and crustal density of 2800 kg/m³ from a standard velocity-density relation [Ludwig *et al.*, 1970]. Other parameters used here are given in Table 1 (also see the appendix). We have found that the Moho Ps phase shows greatest coherence across the array in the 0.1–0.2 Hz frequency range. At these low frequencies, complexities of scattering and other unmodeled phenomena are reduced, simplifying the data and making them more consistent from event to event. We therefore band-pass filter both observed and calculated receiver functions in this frequency range using a zero-phase third-order Butterworth filter before running the grid search. However, it should be noted that our earlier work using unfiltered receiver functions [Sheehan *et al.*, 1992] produced the same general results as those presented here. In addition to the Moho Ps , a significant P -to- S conversion from the base of the Denver Basin is also observed. In the band-pass-filtered receiver functions the effect of the basin is an apparent time lag in the radial P arrival. To address complications due to sedimentary basin conversions such as that from the Denver Basin, the depth to crystalline basement at each station was tabulated from published sources [e.g., Sims, 1985; Sonnenberg, 1987; Burchfiel, 1992; Gries *et al.*, 1992]

Table 1. Receiver Function Results

Station	Latitude, deg	Longitude, deg	Station Elevation, m	^a Average Elevation, m	Basin Depth, km	Crustal Thickness, km	s.d. of Mean	s.d. of Data	N	Depth of Moho Below Sea Level, km
BLA ^b	37.54	-105.58	2469	2550	0.0	49.3	1.8	3.6	4	46.8
BTO	40.38	-105.20	1609	1900	1.4	42.7	1.4	4.3	9	41.1
BUR	39.38	-102.35	1256	1250	1.9	46.7	2.3	4.0	3	45.4
CCR	38.77	-105.22	2807	2530	0.0	47.8	2.7	5.4	4	44.9
CES	39.38	-101.05	965	950	0.0	44.6	0.5	1.4	7	43.6
GRM	39.10	-108.13	2164	2150	2.4	41.7	2.1	5.1	6	39.5
HLD	39.23	-109.08	1452	1770	0.0	43.7	1.6	4.7	9	42.2
KRM	40.13	-106.37	2458	2760	1.8	53.3	1.3	3.6	8	50.8
LED	39.15	-106.36	2879	3250	0.0	49.2	2.2	4.9	5	46.3
LIZ	39.35	-104.54	2030	1900	4.1	51.8	2.8	5.6	4	49.7
LMN	39.41	-103.62	1710	1630	2.9	53.6	2.6	7.3	8	51.9
MON	38.41	-107.99	2097	2330	0.6	47.5	1.9	3.9	4	45.4
ORD	38.50	-103.70	1344	1340	2.0	47.3	1.3	2.3	3	46.0
PAR	38.33	-108.93	1810	2050	4.0	39.3	1.5	3.1	4	37.4
PKS	39.25	-99.53	673	650	0.0	42.9	0.6	1.8	8	42.2
POS	38.54	-106.12	2457	2880	0.0	49.7	3.2	5.5	3	47.2
SOP	39.33	-107.19	2438	2700	0.0	53.6	2.2	5.8	7	51.1
WIG	40.32	-104.07	1368	1430	2.8	50.7	2.4	7.2	9	49.3
WSG	37.77	-104.36	1706	1710	0.7	53.8	2.5	6.2	6	52.1
YUM	40.15	-102.77	1284	1280	2.1	46.0	1.6	4.6	8	44.7

N, total number of events used; s.d. of mean, standard deviation of the mean, s.d. of data, standard deviation of the data.

Parameters used: P velocity of crust, 6.5 km/s; S velocity of crust, 3.76 km/s; density of crust, 2800 kg/m³. P velocity of mantle, 8.0 km/s; S velocity of mantle, 4.62 km/s; density of mantle, 3300 kg/m³. P velocity of sediments, 3.9 km/s; S velocity of sediments, 2.25 km/s; density of sediments, 2300 kg/m³.

^aDiment and Urban [1981].

^bLocal minimum rather than global minimum used

and included in the calculations of synthetic receiver functions. Sensitivity tests of the effect of variations in sedimentary layer thickness and V_p/V_s ratio on the crustal thickness values are given in the appendix.

We have constructed band-passed sections of receiver functions in order to visually examine the correlation of converted phases across the array. An example from a single event is shown in Figure 3, but it should be noted that final results (Table 1) came from the use of three or more events per station. Visualizing the data in pseudo-record section form as shown in the examples in Figures 3 and 4 is more revealing than examining individual receiver functions separately, as phases that correlate across the array become apparent in record section form [e.g., Li *et al.*, 1992; Trehu and Nabelek, 1993]. The Moho P_s arrival is apparent at all stations, constraining travel time through the crust. Phase lags of the initial peak are apparent for stations located on top of thick sedimentary basins (e.g., LIZ, WIG, LMN). The best fitting synthetic receiver functions for a one-dimensional crustal model (sedimentary basin layer is included) are also shown. Synthetic receiver functions were determined for crustal thickness values ranging

from 20 to 75 km (measured from the free surface), and the variations in root-mean-square (RMS) difference between the data and each synthetic show the quality of fit (Figure 4). The best fit crustal thickness found using only this event is approximately 45 km beneath Great Plains stations and increases slightly to the west, to about 50 km. Thicknesses beneath the Rocky Mountains are less well constrained (broader minima) and are only slightly greater than under the Great Plains (recall that depths here are plotted from the surface rather than sea level, so thicknesses under Rockies include up to 2 km of elevation difference). The crust thins farther west, in the Colorado Plateau. Note that the receiver functions and RMS variations shown in Figures 3 and 4 are merely examples for a single event, and the final crustal thicknesses as given in Table 1 come from combining the results from several events (details follow).

By calculating receiver functions and corresponding misfit values for each individual event, we avoid errors that can be introduced by stacking events with different ray parameters. The patterns of the RMS misfit curves are broadly similar for each event (e.g., Figure 5). The final crustal thickness for a given

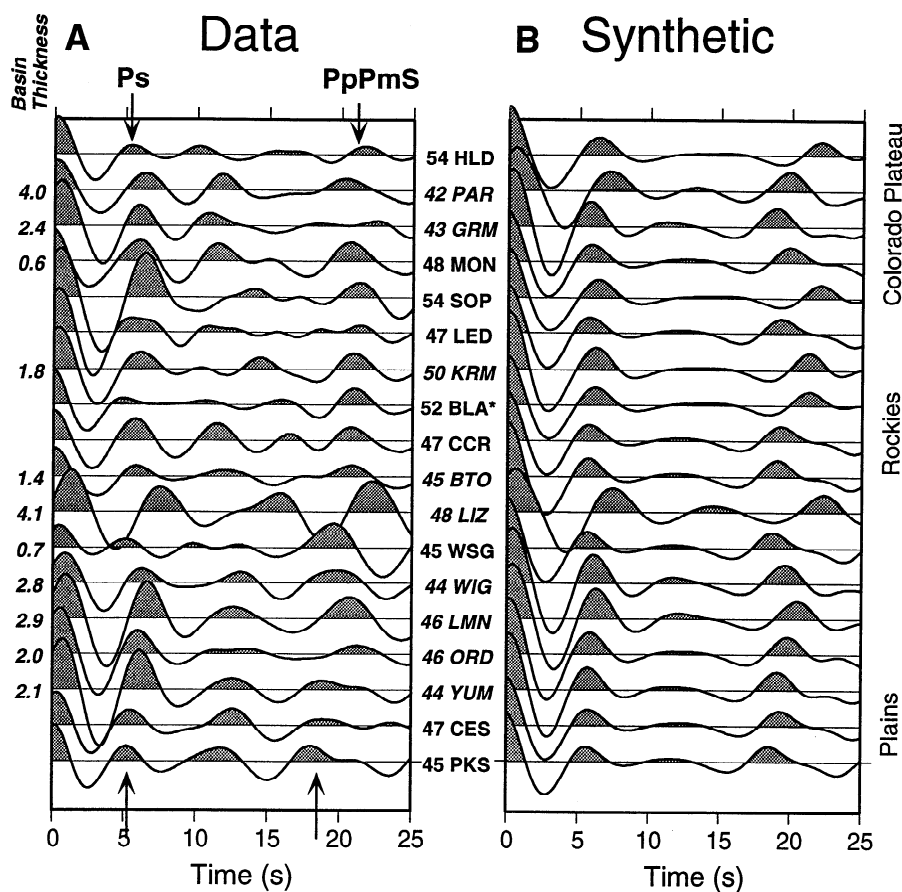


Figure 3. (a) Example of receiver functions from a single event from Hokkaido, Japan, as determined for 18 stations of the Rocky Mountain Front array. Stations are ordered by longitude with westernmost station (HLD) at top. Dominant arrival at 5–6 s is P converted to S at the Moho (P_s). Sedimentary basin thicknesses are indicated at the left. Station names and best fitting crustal thicknesses (measured from surface) are shown in the center of the plot and are italicized for stations with sedimentary basin thickness > 1 km. (b) Example of best fitting synthetic receiver functions for one-dimensional crustal model (sedimentary basin layer is also included) for Hokkaido earthquake. Station name and best fitting crustal thickness (measured from surface) are shown to left. Case where a local, rather than global, minimum was picked identified by asterisk. Variations in sedimentary thickness preclude the simple use of hand timing of P_s phase for determination of crustal thickness, and synthetics which include this layer (as shown here) must be used.

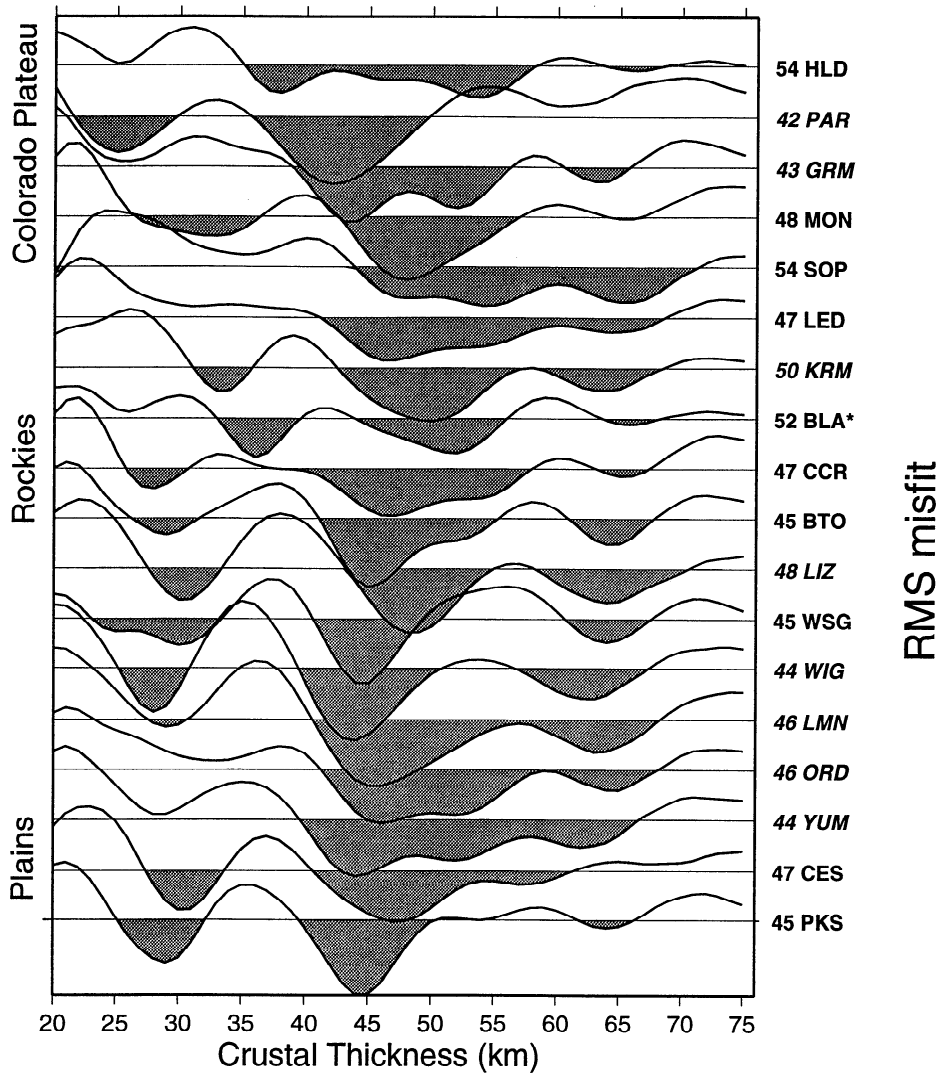


Figure 4. Examples of root-mean-square (RMS) misfit between observed and synthetic receiver functions at Rocky Mountain Front stations calculated for a suite of crustal thicknesses for Hokkaido event. Station where a local, rather than global, minimum was picked in order to maintain consistency between adjacent stations is identified by asterisk. Numbers represent crustal thickness as measured from the surface.

station is determined by (1) calculating the global median of the best fitting thickness values for all events recorded at the station, (2) finding the minimum within 20 km of the global median found in method 1 for each event recorded at the station, and (3) averaging these minima and calculating the standard error. This technique reduces the effect of false minima in the final average thickness. Some correlation on the picks between adjacent stations is imposed by rejecting minima that are far removed from those of adjacent stations if a closer minimum exists (in practice, this was only necessary for station BLA). This procedure is similar to the approach of interpreting arrivals on reflection seismic record sections, which is to focus on phases that are coherent between adjacent common depth point (CDP) gathers and associate them with a common structure. In other words, the correlation across the record section provides information beyond the goodness of fit on any individual trace.

In order to be retained in our final analysis the measured crustal thickness at a given station was required to meet the following criteria: (1) at least three events were used; (2) the

standard deviation of the final crustal thickness is less than 5 km; and (3) the values obtained by normalizing the calculated receiver functions to its RMS value or to the RMS of the data differ by less than 4 km. Crustal thickness values at 20 of the stations studied met these criteria (Table 1). The error estimates given in Table 1 are calculated from the standard deviation of the mean of the individual crustal thickness measurements at a given station from all events. These error estimates reflect the uncertainty in interpreting the receiver functions given the stated assumptions. For example, a change in the assumed crustal velocity would directly change the crustal thickness.

Sensitivity tests which examine crustal thickness variations with changes in several different parameters are explored in the appendix. Our conclusion is that for reasonable variations in parameters we expect individual receiver function estimates to be good to within ~2-4 km if velocities are known. These uncertainties are comparable to the formal uncertainty estimates, which were derived from variations between different events recorded at each station (Table 1).

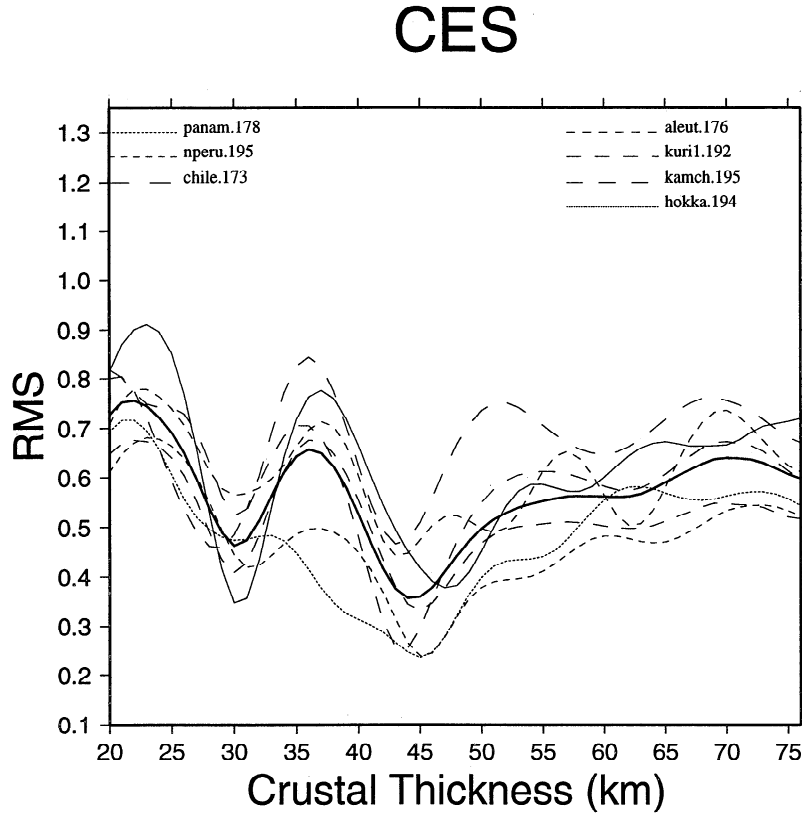


Figure 5. RMS misfit versus crustal thickness for several events recorded at station CES in Western Kansas. Heavy solid line is average of dashed curves. Variously dashed curves represent individual events, as marked. Event abbreviations include event geographic location and julian day (all events in year 1992). The patterns of the RMS curves are broadly similar for each event, with minima at 30 and 45 km.

Isostatic Modeling

Mass Balance Calculations

One critical problem in understanding the compensation of the Rocky Mountains relative to the Great Plains is to separate the isostatic contributions of the crust and mantle to elevation in this region. A simple, first-order constraint can be obtained from the observation that, like much of Earth, relief in the western United States is compensated at a local to regional ($\lesssim 150$ km) scale [Eaton *et al.*, 1978; Jachens *et al.*, 1989]. We show below that this is true for the Rockies. The average elevation of a region in isostatic equilibrium can be considered to be the sum of contributions from the buoyancy of the crust (H_c) and the buoyancy of the mantle (H_m), and if the mean density and thickness of the crust are known, then the buoyancy of the upper mantle can be estimated without inferring mantle densities from seismic velocities. These same techniques have been applied to estimate buoyancy of broad regions of the western United States [Lachenbruch and Morgan, 1990; Jones *et al.*, 1992; Parsons *et al.*, 1994].

Test of Airy root. The Airy root hypothesis can be initially tested by a simple examination of the relationship between observed elevation and Moho depth. For a region supported by Airy isostasy, the mean Moho depth (z_m) should vary linearly with the mean elevation (ϵ) at each station through the equation $z_m = (r_t / \Delta r_m)\epsilon + z_{mREF}$, where r_t is the density of the topography (crust above sea level), Δr_m is the density contrast across the Moho, and z_{mREF} is the crustal

thickness of a section at sea level. Lines relating average elevation (corrected for presence of sediments by reducing the elevation an amount equal to the compaction necessary to make the sediments have the same density of the crust) and Moho depth are shown for $= 35$ km, $r_t = 2700$ kg/m³, and Δr_m as indicated in Figure 6. Note the absence of a linear fit to all the data, indicating that a simple Airy root with a constant Δr_m is impossible. However, a weighted linear fit to points east of 104.6°W , near the western edge of the Great Plains, is good. Points west of 104.6°W are more variable, suggesting other compensation mechanisms.

Constant crustal velocity. In this section we explore several models for interpretation of the receiver function results in terms of compensation of the topography and in the latter part of this section reconcile these isostatic models with gravity anomalies across the Rocky Mountain Front. Since the receiver function only resolves a travel time to a discontinuity, a trade-off between velocity and depth is inherent (Figure A2). The variations in the receiver functions across the Rocky Mountain Front can be interpreted in terms of lateral variations in crustal thickness, crustal velocity, or a combination of both. In the previous section, we assumed a constant crustal velocity based on an average from refraction studies in the region and solved for a depth to the Moho discontinuity. Figure 7a shows the average topography [Diment and Urban, 1981] and inferred Moho depths from our best fitting crustal depth grid search. If we assume a crust with no lateral velocity and density variations and a density contrast of 500

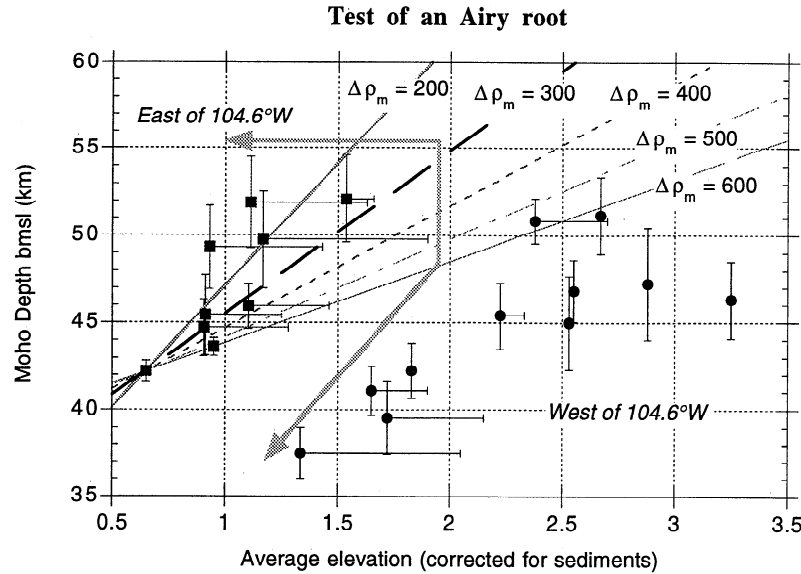


Figure 6. Moho depth versus sediment-corrected elevation. Weighted linear fit to points east of 104.6°W is good (correlation coefficient $R = 0.939$; $z_{m\text{REF}} = 35.7 \pm 1.7 \text{ km}$, $\Delta\rho_m = 300 \pm 70 \text{ kg/m}^3$). Points west of 104.6°W are more variable ($R = 0.807$). Horizontal bar indicates position of data point with sediment effects neglected.

kg/m^3 across the Moho, Airy isostasy requires a 16-km increase in crustal thickness between the easternmost station (PKS) and the region of highest topography (LED) (Figure 7). The crustal thicknesses we obtain using a constant crustal velocity do not show such a large root (Figure 7a); thus we can reject an Airy root as the sole support for the Rockies in the absence of lateral variations in crustal seismic velocities.

We can recover the contribution to the isostatic elevation from the mantle, H_m , using

$$\varepsilon = H_c + H_m - H_0, \quad (5)$$

where ε is the isostatically supported elevation above sea level, H_c and H_m are the amount of topography isostatically supported by the crust and upper mantle, respectively, and H_0 is a reference depth for asthenosphere with no lithosphere above it [Lachenbruch and Morgan, 1990]. The definition of H_c is

$$H_c = \frac{\int_{z=-\varepsilon}^{z=z_m} \rho_a - \rho_c(z) dz}{\rho_a}, \quad (6)$$

where z is depth below sea level, z_m is the depth of the Moho, ρ_a is the asthenospheric density, and $\rho_c(z)$ is the crustal density. The definition of H_m is similar to H_c except that the integration is over mantle depths and in practice we calculate H_m using (5) from ε , H_c , and H_0 . Densities are obtained through the use of a velocity-density relation [Ludwig et al., 1970]. The values of H_m derived from the simple two-layer crustal model (Figure 7a) increase to the west, which implies a significant low-density anomaly in the mantle beneath the Rocky Mountains relative to the Great Plains. The mechanism for this low-density body is not addressed by receiver functions and could be either thermal or compositional in origin. If interpreted in terms of lithospheric thinning with $\rho_m - \rho_a = 50 \text{ kg/m}^3$, where ρ_m is mantle lithospheric density, the H_m values shown predict a lithospheric thickness of nearly 150

km beneath the Great Plains and only 50 km beneath the Rocky Mountains. If interpreted as a bulk change in lithospheric density, this model would require a 1% decrease in average lithospheric density from the Great Plains to the Rocky Mountains, extending to a depth of 170 km. Below 170 km depth, seismic velocity models from surface waves sampling structures east and west of the Rocky Mountain Front are nearly equivalent [Chen and Lerner-Lam, 1993]. However, our H_m values are not tied to any particular mechanism and simply represent an integrated density anomaly.

Compensation confined to crust. A second end-member model is one in which the compensation of the topography is entirely within the crust (Figure 7b), with no compensation permitted from the mantle ($H_m \equiv \text{const}$). Assuming a locally linear relation of density and velocity about $v_c = 6.5 \text{ km/s}$ [Ludwig et al., 1970], we find the single value of average crustal velocity for each longitude that will satisfy both the P_s travel time constraints and assumption of $H_m = \text{const}$. For this calculation, station PKS was chosen as the reference structure with parameters as given in Table 1. In this model, an 18% decrease in average crustal seismic velocity (from 6.5 to 5.5 km/s) is required to both fully compensate 2 km of topography and fit the observed travel times through the crust (Figure 7b). These contrasts are unrealistic, given the minor differences in basement composition between the Rocky Mountains and the Great Plains and, as far as we know, are not seen anywhere in continental interiors [e.g., Braile et al., 1989]. This decrease in seismic velocity beneath the Rocky Mountains would be accompanied by a decrease in the crustal thickness to maintain observed travel time through crust, by approximately 4 km relative to the values in Figure 7a. Hence compensation within the crust would only work if a large decrease in crustal velocities occurred beneath the Rocky Mountains and a corresponding decrease in crustal thickness were present.

Compensation in both crust and mantle. Our last model combines the two end-member models above and includes both lateral variations in crustal velocity and compen-

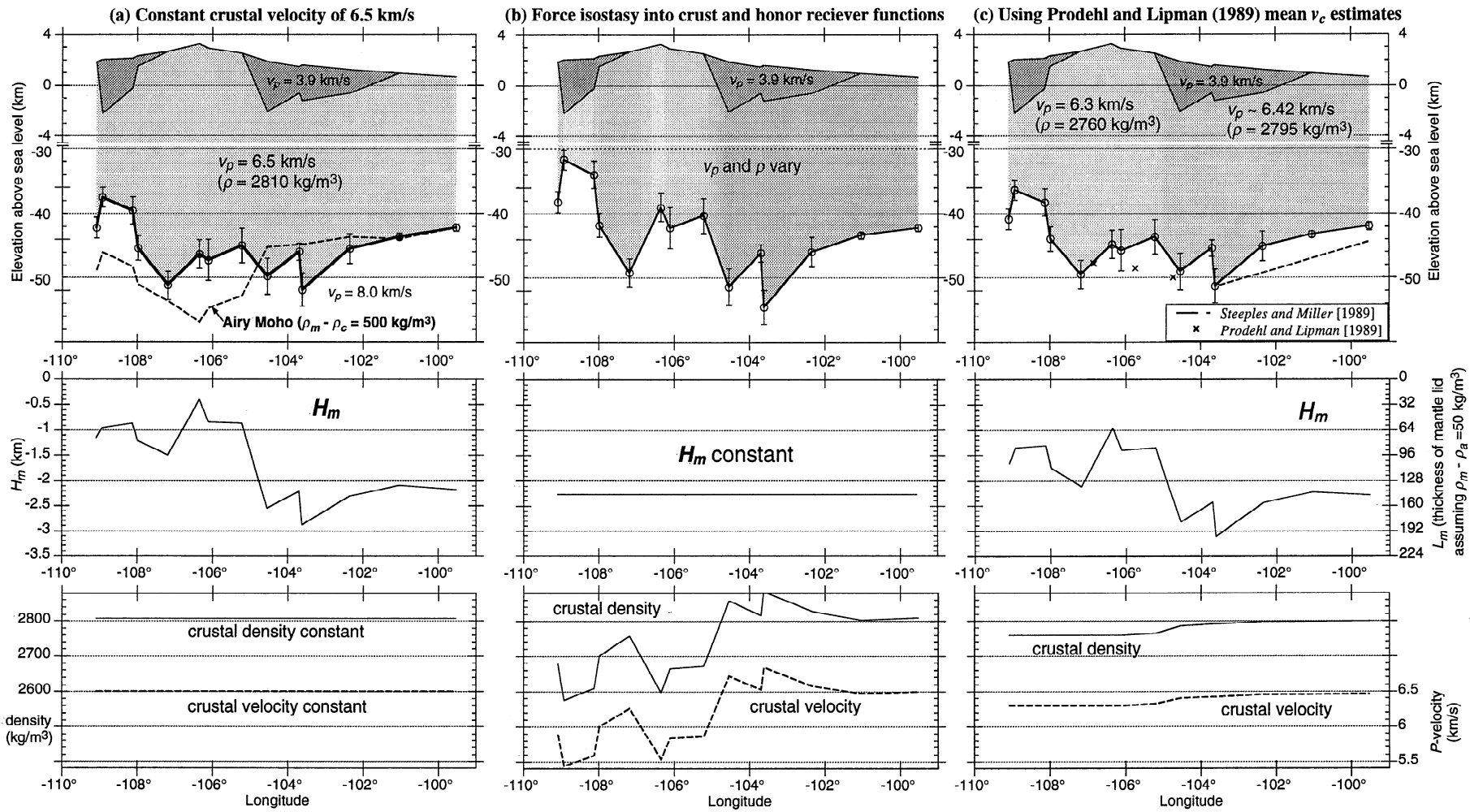


Figure 7. (a) Topography and inferred Moho depths from Table 1. Crustal P velocity is fixed at 6.5 km/s. Points between 38° and 40°N latitude projected into section. Average regional topography from Diment and Urban [1981]. Predicted Airy Moho is shown by dashed line. Solid line in middle panel is H_m [Lachenbruch and Morgan, 1990], the amount of topography that is not isostatically compensated by the crust and must be compensated by the mantle. (b) Topography, inferred Moho depths, and lateral P wave velocity variations for model where all of the isostatic compensation of the Rocky Mountain topography is confined to the crust. H_m is forced equal at all stations. (c) Topography, inferred Moho depths, and lateral P wave velocity variations for model where compensation is accommodated in both the crust and mantle. Moho depths from profiles of Prodehl and Lipman [1989] are shown at selected points projected into profile; Moho from Steeples and Miller [1989] is corrected to same crustal velocities as shown.

sation of the topography accommodated in both the crust and the mantle (Figure 7c). Lateral variations of mean crustal P velocity are taken from the refraction compilation of *Prodehl and Lipman* [1989] and *Braile et al.* [1989]. Our results are in good agreement with those of *Prodehl and Lipman* [1989]. Refraction results from *Steeple and Miller* [1989] corrected to the *Prodehl and Lipman* [1989] mean crustal velocities are also shown in Figure 7c. Reconciliation between the *Steeple and Miller* [1989] and present results can be accommodated by a small decrease in V_p/V_s (increase in V_s) to the east (see the appendix and Figure A2). Our logic in suggesting a decrease in V_p/V_s to the east follows: (1) Increasing V_s will make receiver function thicknesses closer to *Steeple and Miller's* [1989] depth in the plains (this is a decrease in V_p/V_s); (2) no change in V_p/V_s seems necessary to reconcile with *Prodehl and Lipman* [1989] in the Rockies; and (3) the *Lee and Grand* [1994] V_s results coupled with published V_p refraction interpretations [*Prodehl and Lipman*, 1989] indicate lower V_p/V_s in the plains relative to the Rockies. This variation would tend to increase the crustal thicknesses calculated from the receiver functions in the Great Plains relative to areas to the west; thus our discussions of isostasy may in fact minimize the role of the mantle in supporting the topography of the Rocky Mountains. Regardless of whether the *Steeple and Miller* [1989] results are included, the amount of Rocky Mountain topography that must be compensated by the mantle is significantly reduced from the value in Figure 7a. We feel that this model offers the most reasonable reconciliation between the receiver function results, isostatic constraints, and other existing data. If interpreted in terms of variations in the thickness of a constant-density mantle lithosphere, then this model predicts a lid thickness 60 km greater beneath the Great Plains than beneath the Rocky Mountains. The low-density mantle required could be due to either a thermal or compositional mechanism. Interpretations by *Humphreys and Dueker* [1994] based upon P wave tomography suggest a thermal anomaly with partial melting beneath the Rocky Mountains; however, the conjecture that the present elevation of the Rocky Mountains has persisted since Eocene time [*Gregory and Chase*, 1992, 1994] is difficult to reconcile with a single thermal event.

Constraints From Bouguer Anomalies

It is important to reconcile our mass balance models with observed gravity anomalies across the Rocky Mountain Front. The Bouguer gravity anomaly over the Rockies has often been cited, along with the Sierra Nevada of California, as a classic example of Airy compensation [e.g., *Bott*, 1982]. Excellent agreement between observed Bouguer anomalies and those predicted for simple Airy compensation (Figure 8) make an Airy root an attractive explanation, and early seismic refraction interpretations [*Pakiser*, 1963] supported their existence. However, reanalysis and new observations have called into question the presence of the Sierran root [*Jones et al.*, 1994; *Ruppert et al.*, 1994; *Squires and Clayton*, 1994; *Shalev and Malin*, 1994; *Wernicke*, 1994]. Likewise, the receiver function results presented here suggest that a large crustal root does not exist beneath the Rockies. Along our transect, Airy isostasy predicts a ~16-km increase in crustal thickness between the easternmost station and the region of high topography. Even though an Airy root does an excellent job of explaining the gravity data (Figure 8), the seismic data require a more complex scenario with some or all of the compensation taking place in

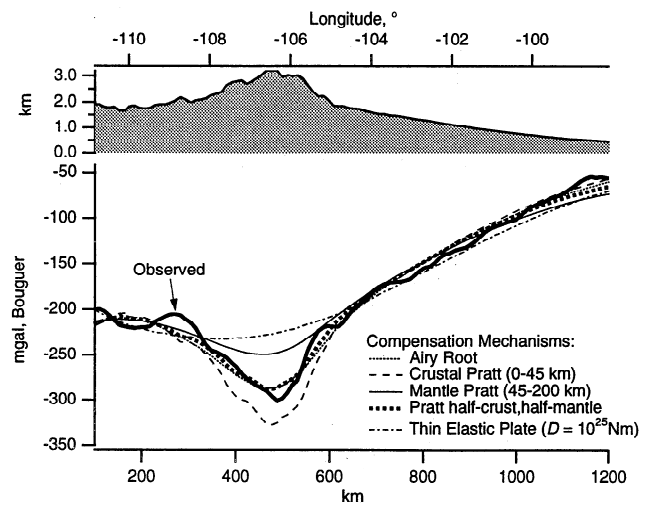


Figure 8. Comparison of Bouguer gravity anomaly across Rockies with isostatically compensated models. (top) Elevations versus longitude, from ETOPO5 gridded topography data, averaged between 38.5 and 40°N. (bottom) Bouguer gravity anomalies, as labeled. Observed gravity is taken from the Decade of North American Geology compilation grid [National Oceanographic and Atmospheric Administration (NOAA), 1989], averaged with latitude in the same manner as topography. Models are calculated assuming a density for topography ρ_t of 2700 kg/m³, a nominal Moho depth z_m of 45 km (corresponding to no topography) and a nominal density contrast across the Moho $\Delta\rho_m$ of 500 kg/m³.

the mantle. Below we describe several gravity models. The gravity models require good spatial sampling of crustal thickness. Our station by station estimates are not closely spaced enough for this purpose, so instead we have made a range of simple gravity models that represent several end-member structures.

One might imagine that the high topography could be supported, in part, by a rigid elastic plate so that the deflection of the Moho is broad and low in amplitude. Such a scenario, implied by coherence studies [*Bechtel et al.*, 1990], could explain the receiver function data but is inconsistent with the Bouguer gravity anomaly. Plate deflections were calculated for a continuous, thin elastic plate [e.g., *Turcotte and Schubert*, 1982] that supports longitudinally averaged topography along an east-west profile. Even a fairly strong plate, with flexural rigidity (D) of 10^{25} N m (corresponds to an elastic plate thickness of over 100 km), shows >10-km increase in depth below the surface between the maximum deflection and the easternmost station PKS, yet it underpredicts the amplitude of the gravity low over the Rockies by 70 mGal (Figure 8). Weaker plates fit the gravity better (although none do better than the Airy root), but they predict even greater relief on the Moho. Hence regional crustal compensation is not a viable explanation for the relatively flat Moho we observe.

Adequate explanations of both seismic and gravity observations are not simple. Mantle compensation by itself predicts a gravity anomaly that is too smooth. The "mantle Pratt" predicted anomaly, in which topography is compensated solely by density changes distributed uniformly between 45 and 200 km depth, under predicts the amplitude of the gravity low. A "crustal Pratt" anomaly similarly over predicts the amplitude of the gravity anomaly (Figure 8). The mean depth of compensation must be somewhere near 50 km and suggests equal parts

of compensation in the crust and mantle (or a very shallow component of mantle compensation). The velocity changes of *Prodehl and Lipman* [1989] (Figure 7c) imply some crustal compensation, so that some fraction of the compensation could occur within the crust. The rest must come from the mantle or from Moho perturbations that are allowed by the receiver function constraints. Such a model has many free parameters, and the nonuniqueness of the gravity field virtually guarantees success in fitting the observed gravity. One example is shown (Figure 8) with compensation evenly partitioned between mantle and crustal density changes. Here depth-averaged mantle densities decrease by 0.7% and crustal densities decrease by 3% beneath the highest topography. This model, with half of the compensation in the crust and half in the mantle, is similar to model used in Figure 7c and fits gravity marginally better than Airy compensation.

Conclusions

The main results of this paper are summarized in Table 1 and Figure 7. The average crustal thicknesses that we find from receiver function analysis are Kansas Great Plains, 43.8 ± 0.4 km and Moho depth of 42.9 km; Colorado Great Plains, 49.9 ± 1.2 km and Moho depth of 48.3 km; Colorado Rocky Mountains, 50.1 ± 1.3 km and Moho depth of 47.4; and northeast Colorado Plateau, 43.1 ± 0.9 and Moho depth of 41.1 at latitudes of $39^\circ \pm 1^\circ\text{N}$. Thus the main changes in crustal thickness observed exist at the transition from the Kansas Great Plains to the Colorado Great Plains and at the transition from the Rocky Mountains to the Colorado Plateau. We do not observe a significant crustal thickness difference between the Colorado Great Plains and the Colorado Rocky Mountains. These results are incompatible with the hypothesis that the compensation of the Rocky Mountains relative to the Great Plains is accommodated purely by an Airy-type crustal root and requires significant support for the topography to come from the mantle. Structures compatible with the receiver functions which restrict compensation to variations in crustal density and thickness are unlikely, as the variations required (18% difference in mean crustal velocity) between the Rocky Mountains and Great Plains are incompatible with a priori information [e.g., *Braile et al.*, 1989; *Prodehl and Lipman*, 1989]. Models with a rigid elastic plate may match receiver function estimates of crustal thickness but underpredict the amplitude of the gravity low over the Rockies. Our favored model includes lateral variations in crustal velocities obtained from refraction studies [*Prodehl and Lipman*, 1989; *Braile et al.*, 1989] and crustal thickness variations constrained by the receiver functions. These models indicate that there is a profound change in mantle density structure near the range front and that it is this density contrast which holds up about half of the mass of the mountains. If interpreted in terms of variations in the thickness of a constant-density mantle lithosphere, then this model predicts a lid thickness 60 km greater beneath the Great Plains than beneath the Rocky Mountains. Future evaluations of *P* and *S* velocities, along with our integrated density constraints, may help resolve the competing thermal and compositional models. Ongoing analyses of the seismic surface wave and body wave data collected in the Rocky Mountain Front experiment are consistent with the existence of low-velocity mantle beneath the Rocky Mountains [e.g., *Lee and Grand*, 1994; *Chen and Lerner-Lam*, 1993] and should shed light on the dimensions and source of this mantle anomaly.

Appendix: Parameter Sensitivity of Grid Search

We conduct a series of tests to better understand the assumptions and limitations of the grid search technique applied here. In all of these tests, we compare observed receiver functions with the best fit synthetic and then perturb one or more of the parameters of interest. For all tests except for the first one, when a parameter is perturbed the inversion is repeated at the new parameter value to find the crustal thickness that gives the best match (in a least squares sense) between observed and calculated receiver functions. Unperturbed values are the same as used in the inversions: crustal *P* wave velocity *V_p* of 6.5 km/s, Poisson's ratio of 0.25 (*V_p/V_s* = 1.73), and sediment *V_p* of 3.9 km/s. Both observed and calculated receiver functions are bandpassed between 0.1 and 0.2 Hz.

Effect of Crustal Thickness

We examine here observed and calculated receiver functions at the easternmost station PKS, representing a simple shield structure. As can be seen (Figure A1a), even a change of 2 km in assumed crustal thickness results in a significant misfit between observed and calculated receiver functions. The misfit is fairly slight at 5 s, when *Ps* arrives, but is most noticeable at 15–25 s, when *PpPmS* and other first reverberations arrive. Hence accurate thicknesses can be determined if the velocities are known, even though the band-pass filtering appears severe.

Effect of *V_p* Variations

To first order, crustal thickness trades off linearly with *V_p*, as shown in Figure A2. The inversions show little sensitivity to *V_p* independent of crustal thickness, so some prior knowledge of *V_p* is useful. The only noticeable sensitivity is the relative amplitude of the first (0 s) pulse to all later pulses, because incidence angle varies with *V_p*. However, other variations in near-surface velocity produce similar effects (e.g., Figure A1C).

Effect of Changing Bulk *V_p/V_s* in Crust

There is a trade-off between *V_p/V_s* and crustal thickness, because both *P* and *S* wave velocities contribute to the timing of the relevant converted phases (Figure A1b). Still for reasonable variations in *V_p/V_s* the crustal thickness estimates change by less than 2 km. The timing between the various first reverberations varies with *V_p/V_s*, seen here between 15 and 27 s, and the observations here favor a value closer to 1.80. However the sensitivity is slight compared to variations between events, and generally we assume *V_p/V_s* = 1.73.

Effect of a Midcrustal Discontinuity

A midcrustal or Conrad discontinuity may contribute to the large arrival near 10–15 s seen at PKS and a few of the other stations (Figure A1a). Calculated receiver functions with an interface near 25 km depth (Figure A1a, bottom trace) fit the observations much better than a single-layer crust, at least at PKS. However, the inclusion of a midcrustal discontinuity would introduce two additional parameters to the inversions, the depth to discontinuity and the velocity contrast across it, which would greatly complicate the evaluation of results. It is also not clear that such an interface is warranted at western stations. We find that for reasonable values of velocities and

Conrad depths the crustal thickness estimates vary by 1 km or less from those determined in a one-layer crust, so we lose little in understanding by ignoring such an interface.

Effect of a Sedimentary Basin

A shallow basin (<5 km deep) introduces a phase lag in the first (0 s) pulse in receiver functions, by interference between direct P and phase conversions at the bottom of the basin (Figure A1c, arrow). The behavior is more complicated for later reverberations, because they must pass through the basin structure two or more times. The phase delays are seen for all records from the Denver Basin and a few at other intermontane basins (Figure 2). For a nominal Vp/Vs of 1.73 within the basin the phase delays are generally underpredicted. The basin depths are generally well known, from other work, and held fixed.

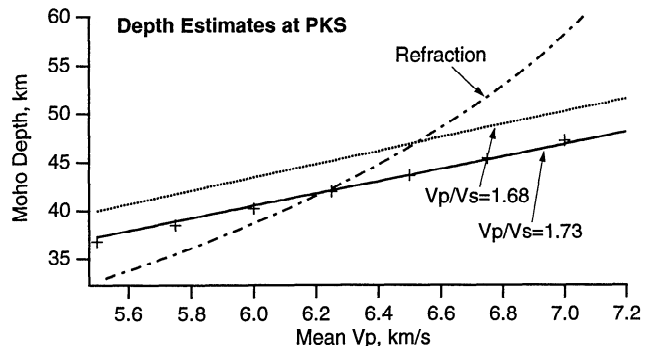
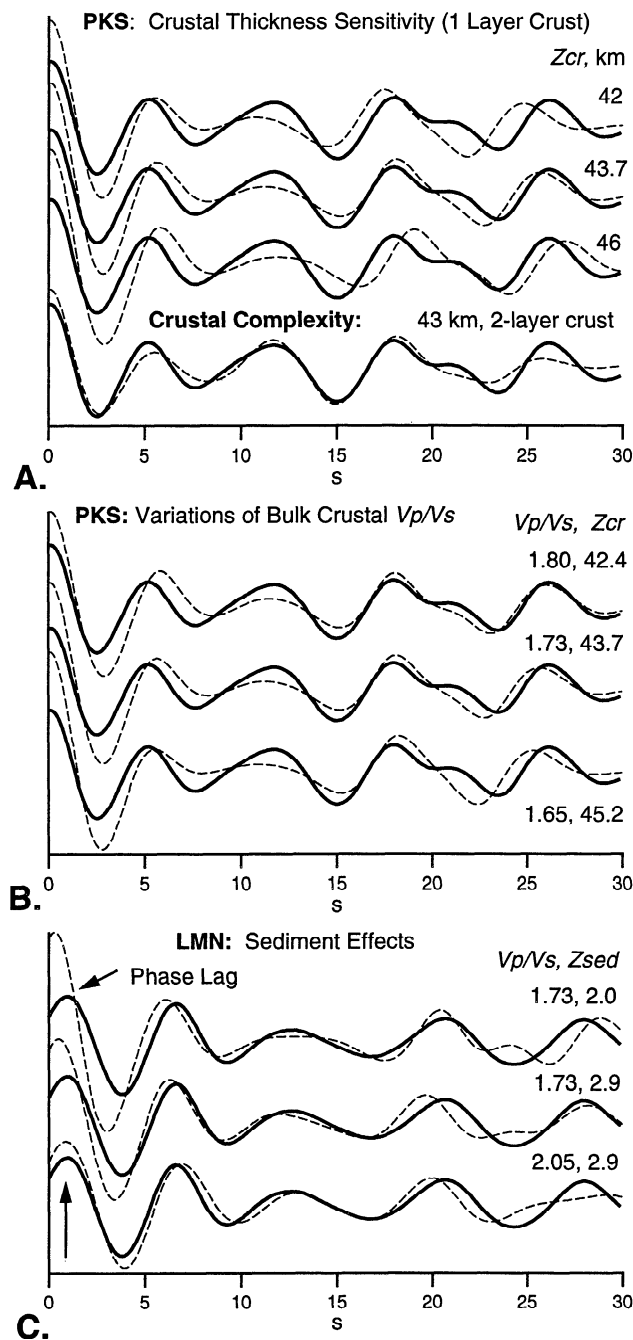


Figure A2. Trade-off between Moho depth estimates and assumed crustal velocity, comparing refraction with receiver function estimates for one-layer crustal models. Trade-off curves are calibrated to observations at station PKS in western Kansas. Solid and dotted lines show receiver function trade-off estimates for two different assumed values of Vp/Vs , assuming that the time delay between P and Ps is constrained so that depth is determined from the Ps delay time and the difference between P and S vertical slowness in the crust. A horizontal slowness of 0.118 s/km is assumed, an average value for the iasp91 travel time curves at teleseismic distances. The pluses show results of actual receiver function inversions for a single event (same event as in Figures 3 and 4) at PKS, for different assumed values of Vp . Dash-dotted line shows comparable results determined from the reversed refraction study of *Steeple and Miller* [1989]. Their travel time slopes and intercept times were assumed to be correct, and standard dipping-interface calculations were done to estimate depth to interface as a function of Vp . The Moho depths were interpolated from the ends of the line to PKS, which lies near the central portion of the line. The two estimates agree for mean crustal velocities near 6.25 km/s, close to the value estimated by *Steeple and Miller* [1989] from PmP observations of 6.2 km/s.

Figure A1. Sensitivity tests of individual receiver functions to significant parameters for Hokkaido event. Thick solid line shows observed receiver function and dashed line shows calculated. Parameters varied include crustal thickness (Zcr , in kilometers), sediment thickness ($Zsed$, in kilometers), and ratio of P -to- S velocity in either crust or sediments (Vp/Vs) and are shown at right. All receiver functions are band-pass-filtered between 0.1 and 0.2 Hz; other parameters given in text. (a) Crustal thickness sensitivity at station PKS. Top three traces show ± 2 km variations in crustal thickness from best fitting value, all other parameters fixed to nominal values. Note significant mismatches, particularly after 15 s. Bottom trace shows one example in which seismograms were calculated for two-layer crust; the midcrustal discontinuity is at 26 km depth with Vp of 6.0 and 6.9 km/s in the upper and lower layer, respectively. Note improved fit between 10 and 15 s. (b) Crustal Poisson's ratio (parameterized as Vp/Vs) is varied over a reasonable range of values, and best fitting crustal thickness is redetermined at station PKS. Quality of fit changes little while Zcr varies by 1.5 km. (c) Assumptions about sedimentary layer are varied for station LMN in Denver Basin. Known basin thickness is 2.9 km (Table 1), corresponding to bottom two traces. Top trace shows effect of a thinner basin. Bottom shows effect of a larger Vp/Vs in sedimentary basin of 2.05. Timing of phase lag of initial peak, arrow, is sensitive to sediment layer properties. In each case the crustal thickness is redetermined. Prominent phase lag observed at LMN is best matched at $Vp/Vs = 2.05$, although crustal thickness changes by less than 3 km in response to each perturbation shown.

Effect of V_p/V_s Variations in Shallow Sediments

Porous sediments can be very inefficient transmitters of shear waves, and anomalously high V_p/V_s ratios may occur in shallow basins [e.g., King, 1966; Press, 1966]. Receiver functions from stations in the Denver Basin are best explained by V_p/V_s of 2.0-2.1 (Figure A1c, bottom). Increasing V_p/V_s increases the phase delay of the initial pulse, reduces its amplitude to be closer to what we observe, and decreases crustal thickness. The crustal thickness varies by less than 3 km for each of the tests shown. The effect is particularly strong at LIZ, which overlies the deepest part of the Denver Basin, and the large uncertainties here may be an indication that unusual basin effects may be important.

Overall, our conclusion is that the effects discussed here result in 2-4 km uncertainties in crustal thickness estimates for reasonable variations in parameters. These uncertainties are comparable to the formal uncertainty estimates, which were derived from variations between different events recorded at each station (Table 1). Hence we consider the lack of a large root beneath the high Rockies to be a robust feature of these observations.

Acknowledgments. We are grateful to those who participated in the field work and data management associated with the Rocky Mountain Front PASSCAL experiment, including Steve Grand, Eugene Humphreys, Sean Chen, Ken Dueker, Duk Lee, Randy Palmer, Hong-Sheng Guo, Jacob Lawrence, David Jones, Jim Gaherty, and Steve Shapiro. We thank the PASSCAL Instrument Center at Lamont for providing instruments and field support. We thank Jim Pechmann, Steve Taylor, and an anonymous associate editor for constructive reviews which helped improve the paper and Martha Savage and Ken Dueker for comments on various drafts. Jennifer Crews tabulated the depth-to-basement at each station. Figures 3-5 were made with GMT software, provided free of charge by Paul Wessel and Walter Smith [Wessel and Smith, 1991]. A.F.S was supported by a Lamont Postdoctoral Fellowship during the initial stages of this work. This research was supported by National Science Foundation grants EAR-9018424, 9305282, and EAR-9319008. Lamont-Doherty contribution 5369.

References

- Abers, G. A., X. Hu, and L. R. Sykes, Source scaling of earthquakes in the Shumagin region, Alaska: Time domain inversions of regional waveforms, *Geophys. J. Int.*, in press, 1995.
- Ammon, C. J., G. E. Randall, and G. Zandt, On the nonuniqueness of receiver function inversions, *J. Geophys. Res.*, 95, 15,303-15,318, 1990.
- Axelrod, D. I., and H. P. Bailey, Tertiary vegetation, climate, and altitude of the Rio Grande depression, New Mexico-Colorado, *Paleobiology*, 2, 235-254, 1976.
- Bechtel, T. D., D. W. Forsyth, V. L. Sharpton, and R. A. F. Grieve, Variations in effective elastic thickness of the North American lithosphere, *Nature*, 343, 636-638, 1990.
- Bird, P., Laramide crustal thickening event in the Rocky Mountain foreland and Great Plains, *Tectonics*, 3, 741-758, 1984.
- Bird, P., Formation of the Rocky Mountains, western United States-A continuum computer model, *Science*, 239, 1501-1507, 1988.
- Bott, M. H. P., *The Interior of the Earth: Its Structure, Constitution and Evolution*, 403 pp., Elsevier, New York, 1982.
- Braile, L. W., W. J. Hinze, R. R. B. von Frese, and G. R. Keller, Seismic properties of the crust and uppermost mantle of the conterminous United States and adjacent Canada, in *Geophysical Framework of the Continental United States*, edited by L. C. Pakiser and W. D. Mooney, *Mem. Geol. Soc. Am.*, 172, 655-680, 1989.
- Burchfiel, B. C., Tectonostratigraphic map of the Cordilleran Orogen belt: Conterminous United States, in *The Geology of North America*, vol. G3, *The Cordilleran Orogen: Conterminous United States*, edited by B. C. Burchfiel, P. W. Lipman, and M. L. Zoback, *Geol. Soc. Am. Boulder, Colo.*, 1992.
- Burchfiel, B. C., D. S. Cowan, and G. A. Davis, Tectonic overview of the Cordilleran orogen in the western United States, in *The Geology of North America*, vol. G3, *The Cordilleran Orogen: Conterminous United States*, edited by B. C. Burchfiel, P. W. Lipman, and M. L. Zoback, *Geol. Soc. Am.*, pp. 407-479, Boulder, Col., 1992.
- Chen, Q., and A. Lerner-Lam, Where is the western edge of the North American Craton?, *Eos Trans. AGU*, 74(43), Fall Meet. Suppl., 423, 1993.
- Clayton, R. W., and R. A. Wiggins, Source shape estimation and deconvolution of teleseismic bodywaves, *Geophys. J. R. Astron. Soc.*, 47, 151-177, 1976.
- Dickinson, W. R., M. A. Klute, M. J. Hayes, S. U. Janecke, E. R. Lundin, M. A. Mekittrick, and M. D. Olivares, Paleogeographic and paleotectonic setting of Laramide sedimentary basins in the central Rocky-Mountain region, *Geol. Soc. Am. Bull.*, 100, 1023-1039, 1988.
- Diment, W. H., and T. C. Urban, Average elevation map of the conterminous United States (Gilluly averaging method), *U.S. Geol. Surv. Geophys. Invest. Map, GP-933*, 1981.
- Eaton, G. P., A tectonic redefinition of the southern Rocky Mountains, *Tectonophysics*, 132, 163-193, 1986.
- Eaton, G. P., Topography and origin of the southern Rocky Mountains and Alvarado Ridge, in *Continental Extensional Tectonics*, edited by M. P. Coward, J. F. Dewey, and P. L. Hancock, *Geol. Soc. Spec. Publ. London*, 28, 355-369, 1987.
- Eaton, G. P., R. R. Wahl, H. J. Prostka, D. R. Mabey, and M. D. Kleinkopf, Regional gravity and tectonic patterns: Their relation to late Cenozoic epeirogeny and lateral spreading in the western Cordillera, *Mem. Geol. Soc. Am.*, 152, 51-91, 1978.
- Epis, R. C., and C. E. Chapin, Geomorphic and tectonic implications of the post-Laramide, late Eocene erosion surface in the southern Rocky Mountains, in *Cenozoic History of the Southern Rocky Mountains*, edited by B. F. Curtis, *Mem. Geol. Soc. Am.*, 144, 45-74, 1975.
- Grand, S. P., and D. V. Helmberger, Upper mantle shear structure of North America, *Geophys. J. R. Astron. Soc.*, 76, 399-438, 1984.
- Gregory, K. M., and C. G. Chase, Tectonic significance of paleobotanically estimated climate and altitude of the late Eocene erosion surface, Colorado, *Geology*, 20, 581-585, 1992.
- Gregory, K. M., and C. G. Chase, Tectonic and climatic significance of a late Eocene low-relief, high-level geomorphic surface, Colorado, *J. Geophys. Res.*, 99, 20140-20160, 1994.
- Gries, R., J. C. Dolson, and R. G. H. Reynolds, Structural and stratigraphic evolution and hydrocarbon distribution, Rocky Mountain foreland, in *Foreland Basins and Fold Belts*, edited by R. W. MacQueen and D. A. Leckie, *AAPG Mem.*, 55, 395-425, 1992.
- Gurrola, H., J. B. Minster, and T. Owens, The use of velocity spectrum for stacking receiver functions and imaging upper mantle discontinuities, *Geophys. J. Int.*, 117, 427-440, 1994.
- Gurrola, H., G. E. Baker, and J. B. Minster, Simultaneous time domain deconvolution with application to the computation of receiver functions, *Geophys. J. Int.*, 120, 537-543, 1995.
- Humphreys, E. D., and K. G. Dueker, Physical state of the western U.S. upper mantle, *J. Geophys. Res.*, 99, 9635-9650, 1994.
- Jachens, R. C., R. W. Simpson, R. J. Blakely, and R. W. Saltus, Isostatic residual gravity and crustal geology of the United States, in *Geophysical Framework of the Continental United States*, edited by L.C. Pakiser and W. D. Mooney, *Mem. Geol. Soc. Am.*, 172, 405-424, 1989.
- Jones, C. H., B. P. Wernicke, G. L. Farmer, J. D. Walker, D. S. Coleman, L. W. McKenna, and F. V. Perry, Variations across and along a major continental rift: An interdisciplinary study of the Basin and Range Province, western USA, *Tectonophysics*, 213, 54-84, 1992.
- Jones, C. H., H. Kanamori, and S. W. Roecker, Missing roots and mantle "drips": Regional Pn and teleseismic arrival times in the southern Sierra Nevada and vicinity, California, *J. Geophys. Res.*, 99, 4567-4601, 1994.
- King, M. S., Wave velocities in rocks as a function of changes in overburden pressure and pore fluid saturants, *Geophysics*, 31, 50-73, 1966.
- Lachenbruch, A. H., and P. Morgan, Continental extension, magmatism and elevation: formal relations and rules of thumb, *Tectonophysics*, 174, 39-62, 1990.
- Langston, C.A., Corvallis, Oregon, crustal and upper mantle receiver structure from teleseismic P and S waves, *Bull. Seismol. Soc. Am.*, 67, 713-724, 1977.
- Langston, C.A., Structure under Mount Rainier, Washington, inferred from teleseismic bodywaves, *J. Geophys. Res.*, 84, 4749-4762, 1979.

- Langston, C.A., Evidence for subducting lithosphere under southern Vancouver Island and western Oregon from teleseismic P wave conversions, *J. Geophys. Res.*, 86, 3857-3866, 1981.
- Langston, C. A., Scattering of teleseismic body waves under Pasadena, California, *J. Geophys. Res.*, 94, 1935-1951, 1989.
- Lee, D.-K., and S. P. Grand, Mantle shear structure beneath the Colorado Rocky Mountains, *Eos Trans. AGU*, 75(44), Fall Meet. Suppl., 485, 1994.
- Li, X.-Q., J. Nabelek, and G. Zandt, Geometry of subducted Juan de Fuca plate beneath western Oregon from broadband receiver function studies, *Eos Trans. AGU*, 73(43), Fall Meet. Suppl., 391, 1992.
- Lipman, P. W., Magmatism in the Cordilleran United States; Progress and problems, in *The Geology of North America*, vol. G3, *The Cordilleran Orogen: Conterminous United States*, edited by B. C. Burchfiel, P. W. Lipman, and M. L. Zoback, Geol. Soc. of Am., pp. 481-514, Boulder, Col., 1992.
- Lipman, P. W., H. J. Prostka, and R. L. Christiansen, Evolving subduction zones in the western United States, as interpreted from igneous rocks, *Science*, 174, 821-825, 1971.
- Livaccari, R. F., Role of crustal thickening and extensional collapse in the tectonic evolution of the Sevier-Laramide orogeny, western United States, *Geology*, 19, 1104-1107, 1991.
- Ludwig, W. J., J. E. Nafe, and C. L. Drake, Seismic refraction, in *The Sea*, vol. 4, *Ideas and Observations on Progress in the Study of the Seas*, edited by A. E. Maxwell, pp. 53-84, Wiley-Intersci., New York, 1970.
- MacGinitie, H. D., Fossil plants of the Florissant beds, Colorado, *Carnegie Inst. Washington Publ.*, 599, 198 pp., 1953.
- Molnar, P., and H. Lyon-Caen, Some simple physical aspects of the support, structure, and evolution of mountain belts, in *Processes in Continental Lithospheric Deformation*, edited by S. P. Clark, B. C. Burchfiel, and J. Suppe, *Spec. Pap. Geol. Soc. Am.* 218, 179-207, 1988.
- National Oceanographic and Atmospheric Administration (NOAA), DNAG compilation, Silver Spring, Md., 1989.
- Owens, T. J., and R. S. Crosson, Shallow structure effects on broad-band teleseismic P waveforms, *Bull. Seismol. Soc. Am.*, 78, 96-108, 1988.
- Owens, T. J., G. Zandt, and S. R. Taylor, Seismic evidence for an ancient rift beneath the Cumberland Plateau, Tennessee: A detailed analysis of broadband teleseismic P waveforms, *J. Geophys. Res.*, 89, 7783-7795, 1984.
- Owens, T. J., S. R. Taylor, and G. Zandt, Crustal structure at regional seismic test network stations determined from inversion of broadband teleseismic P waveforms, *Bull. Seismol. Soc. Am.*, 77, 631-662, 1987.
- Owens, T. J., R. S. Crosson, and M. A. Hendrickson, Constraints on the subduction geometry beneath western Washington from broad-band teleseismic waveform modeling, *Bull. Seismol. Soc. Am.*, 78, 1319-1334, 1988.
- Pakiser, Structure of the crust and upper mantle in the western United States, *J. Geophys. Res.*, 68, 5747-5756, 1963.
- Parsons, T., G. A. Thompson, and N. H. Sleep, Mantle plume influence on the Neogene uplift and extension of the U.S. western Cordillera, *Geology*, 22, 83-86, 1994.
- Phinney, R. A., Structure of the Earth's crust from spectral behavior of long-period waves, *J. Geophys. Res.*, 69, 2997-3017, 1964.
- Press, F., Seismic velocities, in *Handbook of Physical Constants*, edited by S. P. Clark, *Memoir Geol. Soc. Am.*, 97, 195-218, 1966.
- Prodehl, C., and P. W. Lipman, Crustal structure of the Rocky Mountain region, in *Geophysical Framework of the Continental United States*, edited by L. C. Pakiser, and W. D. Mooney, *Mem. Geol. Soc. Am.*, 172, 249-284, 1989.
- Ruppert, S. R., L. J. Squires, R. Keller, Lithospheric structure beneath the southern Sierra Nevada region and southern Basin and Range, *Eos Trans. AGU*, 75(44), Fall Meet. Suppl., 584, 1994.
- Shalev, E., and P. E. Malin, Moho map of the eastern central California, *Eos Trans. AGU*, 75(44), Fall Meet. Suppl., 584-585, 1994.
- Sheehan, A. F., J. A. Lawrence, G. A. Abers, Q. Chen, and A. L. Lerner-Lam, Crustal thickness variations across the Rocky Mountain Front from teleseismic receiver functions, *Eos Trans. AGU*, 71(43), Fall Meet. Suppl., 372, 1992.
- Sipkin, S. C., and A. L. Lerner-Lam, Pulse-shape distortion introduced by broadband deconvolution, *Bull. Seismol. Soc. Am.*, 82, 238-258, 1992.
- Sims, P. K., Precambrian basement map of the northern midcontinent, U.S.A., *U.S. Geol. Surv. Map I-1853-A*, 16 pp., 1985.
- Sonnenberg, S. A., Tectonic, sedimentary, and seismic models for D Sandstone, Zenith Field area, Denver Basin, Colorado, *AAPG Bull.*, 71, 1366-1377, 1987.
- Squires, L. J., and R. W. Clayton, The crust beneath the Sierra Nevada from dense refraction data, *Eos Trans. AGU*, 75(44), Fall Meet. Suppl., 584, 1994.
- Steebles, D. W., and R. D. Miller, Kansas refraction profiles, in *Geophysics in Kansas*, *Kansas Geol. Surv. Bull.*, 226, 129-164, 1989.
- Trehu, A., and J. Nabelek, Imaging the lithosphere from above, below and within: An example from the Cascadia subduction zone beneath central Oregon, paper presented at IRIS Annual Meeting, Incorporated Research Institutions for Seismology (IRIS), Waikaloa, Hawaii, 1993.
- Turcotte, D. L., and G. Schubert, *Geodynamics: Applications of Continuum Physics to Geological Problems*, 450 pp., John Wiley, New York, 1982.
- Wernicke, B., Crustal mass balance in Central Basin and Range: The Sierran root problem, *Eos Trans. AGU*, 75(44), Fall Meet. Suppl., 583, 1994.
- Wessel, P., and W. H. F. Smith, Free software helps map and display data, *Eos Trans. AGU*, 72, 441, 445-446, 1991.

G. A. Abers, Department of Geology, University of Kansas, Lawrence, KS 66044.

C. H. Jones and A. F. Sheehan, Campus Box 216, CIRES, University of Colorado, Boulder, CO 80309. (e-mail: afs@mantle.colorado.edu)

A. L. Lerner-Lam, Lamont-Doherty Earth Observatory, Palisades, NY 10964.

(Received July 11, 1994; revised June 16, 1995; accepted June 20, 1995.)